# Study on Ti fiber reinforced TiAl$_3$ composite by infiltration-in situ reaction

**Y. M. Liu · Z. Y. Xiu · G. H. Wu · W. S. Yang ·**
**G. Q. Chen · H. S. Gou**

**Abstract** This study is concerned with investigation of forming Ti fiber reinforced TiAl$_3$ composite by infiltration-in situ reaction. The as-cast material was obtained by pressing molten pure Al into a preform which was composed of Ti particles and Ti fibers. Based on the differential scanning calorimetry (DSC) result, in situ reaction samples were obtained by heating as-cast materials to 660, 950, and 1300 °C, and held for 1 h, respectively. The microstructure evolution of in situ reaction samples was analyzed by scanning electron microscope and Energy dispersive X-ray (EDX). In addition, the phase composition of products was inspected by X-ray diffraction (XRD). Experiment results show that TiAl$_3$ was formed initially, which was the unique product between Ti and Al. While at high temperature, products of Ti fibers and Al were complex, and Ti$_x$Al$_{1-x}$ ($0.25 < x < 0.75$) compounds were formed around Ti fibers. Finally, TiAl$_3$ decomposed, and oxidation occurred. The mechanism of in situ reaction between Ti and Al in this system was discussed.

Y. M. Liu · G. H. Wu (✉) · W. S. Yang ·
G. Q. Chen · H. S. Gou
School of Materials Science and Engineering,
Harbin Institute of Technology, P.O. Box 3023, Science Park,
No. 2 Yikuang Street, Harbin, Heilongjiang 150080,
People's Republic of China
e-mail: wugh@hit.edu.cn

Y. M. Liu
e-mail: lym-1980@126.com

Z. Y. Xiu
Research Academy of Science and Industry Technology,
Harbin Institute of Technology, P.O. Box 3023, Science Park,
No. 2 Yikuang Street, Harbin, Heilongjiang 150080,
People's Republic of China

## Introduction

Titanium aluminide compounds (Ti$_3$Al, TiAl, TiAl$_3$) have been investigated extensively as potential high temperature structural materials [1, 2]. This is due to their outstanding engineering performances, such as excellent acid/alkali corrosion resistance, high specific modulus and strength [3]. Especially TiAl$_3$ has many attractive characteristics such as low density ($\sim$3.3 g/cm$^3$), high hardness and high melting temperature ($\sim$1390 °C). However, the intrinsic low tensile ductility at room temperature and poor high temperature strength has limited its application [4, 5]. Alloying with fourth-period transition elements (such as Cr, Mn, Fe and Co) and reinforcing with particles (such as TiC, TiB$_2$, TiN) which have not resulted in great improvement of ductility at room temperature [6–8].

Recently, the introduction of long fiber reinforcements in these compounds might overcome the disadvantage [9–11]. The reinforcement is often silicon carbide (SiC/C) monofilaments with a thin carbon protective coating. However, above 800 °C, the carbon protective coating of the continuous reinforcement tends to react with matrix during consolidation, leading to deterioration of mechanical and physical properties of resulting composites [12, 13]. It was stated by Zhang et al. [14] that TiNb fiber could be introduced into titanium aluminide matrix by using a hot-pressed fabrication technology. On the other hand, He and Hu [15] studied a Ti alloy matrix composite with Ti fiber reinforcement and investigated the interface reactant between fibers and the matrix.

The present study suggests a new way to fabricate TiAl$_3$ matrix composite (Ti fiber as a reinforcement) by infiltration-in situ reaction technology. The microstructure evolution, and phase formation were analyzed, and reaction mechanism was investigated.

## Materials and experimental methods

Ti fiber reinforced TiAl$_3$ composite which was prepared by infiltration-in situ reaction method. Ti particles (38 μm in diameter), Ti fibers (120 μm in diameter), and pure Al were used as raw materials. The nominal composition of Ti particles and Ti fibers is shown in Table 1. The stoichiometric ratio of Ti particles to Al was about 1:3, and the volume fraction of Ti fibers was about 35%.

Ti fibers were coated by Ti particles, and coated fibers were aligned in a steel mold. Molten pure Al was pressed into the mold, and then the mold cooled rapidly, subsequently, the as-cast material was obtained.

Ti and Al (Ti fiber and Al, as well as Ti particle and Al) in situ reaction sequence was studied by differential scanning calorimetry (DSC). The as-cast sample was heated to 1400 °C, at a rate of 10 °C/min, in an STA 449C DSC. Based on the DSC result (there were exothermic peaks at 660, 950, and 1300 °C), as-cast samples were heated to 660, 950, and 1300 °C, and held for 1 h at different temperature, respectively. Reaction temperatures were accurate to ±5 °C.

An S-4700 scanning electron microscopy (SEM) was used for morphology examination. Energy dispersive X-ray (EDX) was used to identify and calculate the approximate elemental composition of products. X-ray diffraction (XRD) was performed using Philips X'pert X-ray diffraction device for phase analysis, and the patterns were compared with standard spectra from powder diffraction files.

## Results and discussion

### As-cast composite

Figure 1 shows the SEM microstructure and the corresponding XRD pattern of as-cast composites. The micrograph indicates that a thin reaction layer (an average thickness of 2 μm) was formed between Ti fiber and Al (Fig. 1a). EDX result shows that this product was TiAl$_3$ (the atomic ratio of Ti:Al was about 1:3), and a thin layer (∼ 2 μm) of TiAl$_3$ phase was also formed between Ti particles and Al.

Formation of TiAl$_3$ was also confirmed by XRD (Fig. 1b). TiAl$_3$ diffraction pattern was observed besides the Ti and Al patterns (they are raw materials), which indicates the interface reactant of Ti and Al was formed.

### DSC curve

Figure 2 shows the DSC curve of as-cast materials. An exothermic peak at about 653 °C was recorded. Subsequently, an endothermic peak at about 656 °C was detected, which indicates the melting of Al. Following the endothermic peak, a sharp exothermic peak at about 660 °C can be observed. By heating the as-cast material to high temperature, other two exothermic peaks can be seen (at about 950 and 1300 °C, respectively).

In order to understand the characteristics of microstructure evolution and phase transformation during in situ

**Table 1** Nominal composition of Ti particle and Ti fiber

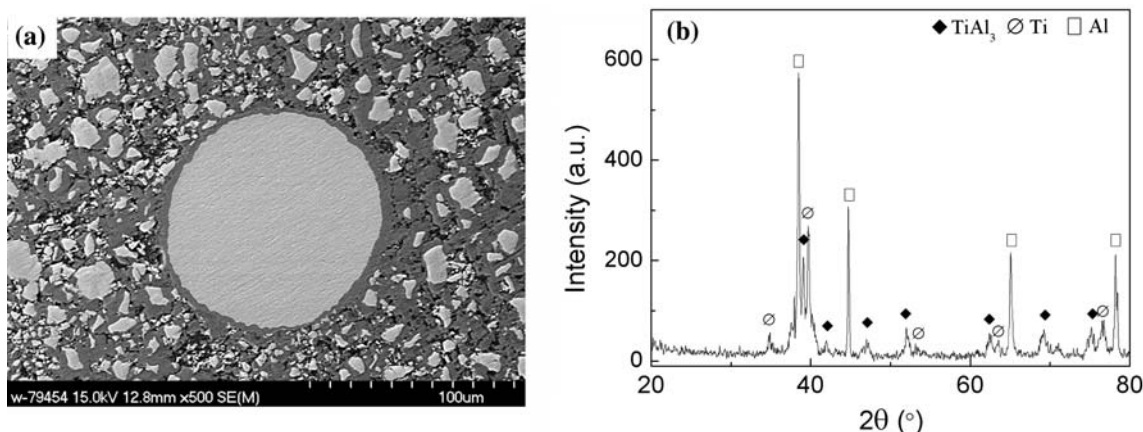| Composition (at.%) | Fe | Si | O | N | H | V | Al | Ti |
|---|---|---|---|---|---|---|---|---|
| Ti particle | 0.056 | 0.026 | 0.63 | 0.054 | 0.051 | – | – | 99.183 |
| Ti fiber | – | – | – | – | – | 1.13 | 7.46 | 91.41 |



**Fig. 1** **a** SEM micrograph of the as-cast composite, **b** XRD pattern of the as-cast composite
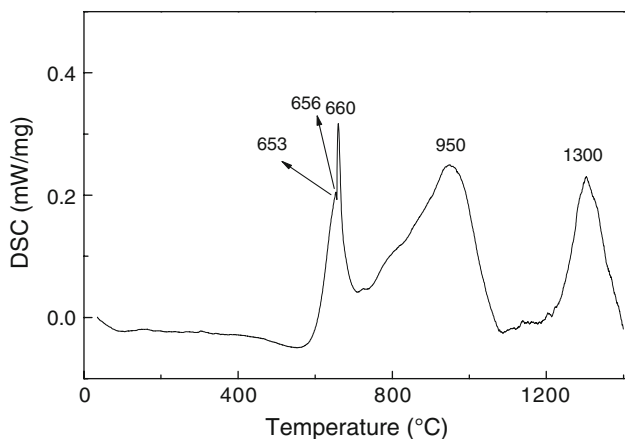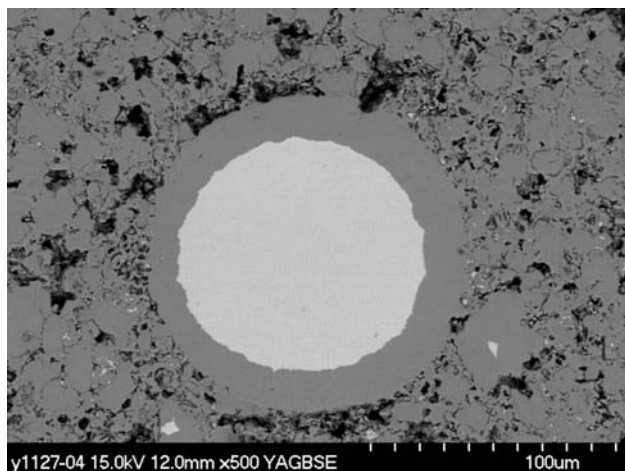
**Fig. 2** DSC curve of the as-cast composite



**Fig. 3** SEM micrograph of in situ reaction composites at 660 °C

reaction, as-cast materials were heated to three different temperatures of 660, 950, and 1300 °C (based on the DSC result), and held for 1 h, respectively.

In situ reaction composite

When the as-cast material was heated to 660 °C and held for 1 h, the SEM image was shown in Fig. 3. It is obvious that the thickness of reacting layer around Ti fiber increased. At the same time, the reacting layer thickness also increased between Ti particles and Al.

The extent of reaction increased with increasing temperature. Figure 4a is the SEM image of as-cast sample was held at 950 °C for 1 h, in which there were four sequential layers around Ti fiber. An expanded view of the interface between Ti fiber and Al was shown in Fig. 4b, which marked with A, B, C, D, and E in different atomic number contrast. The element concentrations at different positions were measured by EDX, as illustrated in Fig. 5. From "A" to "E", Ti and V decreased, while Al increased.

While at this stage, Ti particles eliminated, and lumpy shaped particles were formed. Higher magnification SEM photographs of the matrix in Fig. 4a was shown in Fig. 4c. EDX indicates that these particles were $TiAl_3$. Some white
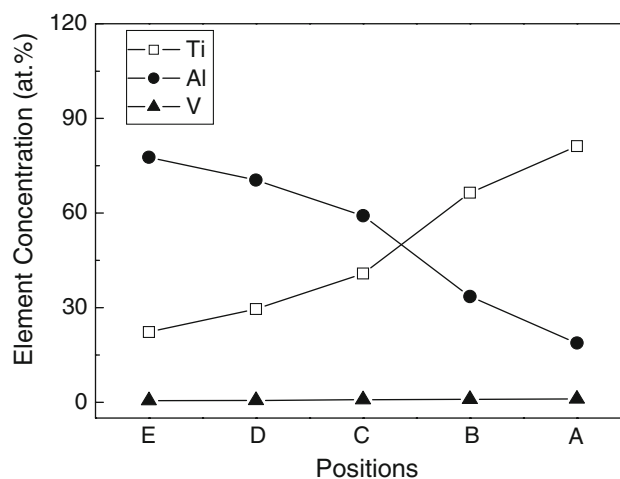


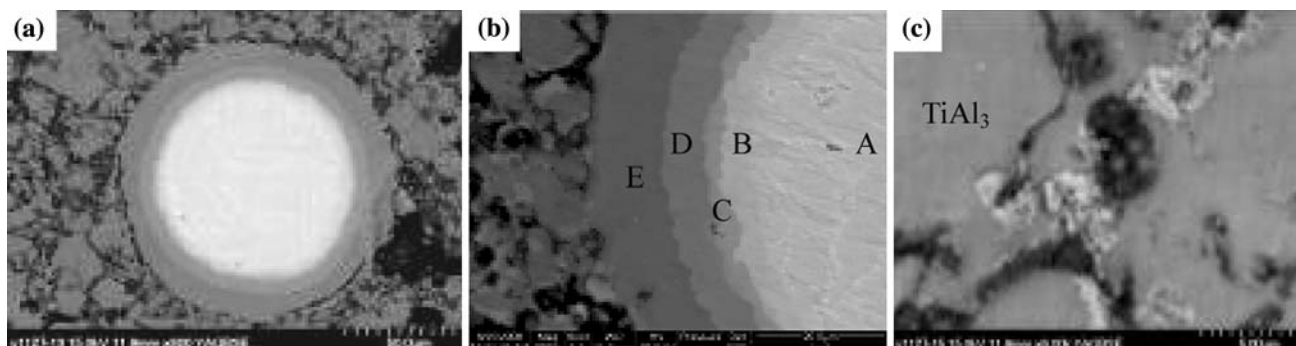**Fig. 5** Chemical composition of different positions in Fig. 4



**Fig. 4** SEM micrograph of in situ reaction composites at 950 °C. **a** Low magnification of Ti fiber and the matrix, **b** high magnification of Ti fiber, **c** high magnification of the matrix

products were observed around these lumpy particles. These white products were composed of Ti, Al, and O (Ti 27.55%, Al 53.03%, O 19.4%), which implies that oxidation occurred at this temperature.

At 1300 °C, the thickness of reacting layers around Ti fiber increased (Fig. 6a), and the element concentrations at different positions (Fig. 6b) were shown in Fig. 7. From "F" to "J", Ti and V decreased, while Al increased.

$TiAl_3$ in the matrix decomposed, and islands $TiAl_3$ phases and rodlike shape particles (Ti 42.91%, Al 26.81%, O 30.27%) formed. The higher magnification SEM photograph was shown in Fig. 6c.

Figure 8 shows XRD patterns of in situ reaction samples. When the sample was held at 660 °C for 1 h, there were $TiAl_3$ and Ti phases (mainly Ti fiber from SEM observation) without Al diffraction peaks. With an increase in temperature, at 950 °C, $Al_2O_3$ and $Ti_4O_7$ XRD patterns were generated, besides the formation of $TiAl_3$. At 1300 °C, the intensity of $TiAl_3$ peaks decreased, but the relative intensity of $TiO_2$ and $Al_2O_3$ increased.

In addition, it is noted that multiphase products of Ti–Al compounds (besides $TiAl_3$) around Ti fiber are observed by SEM, but they have not been detected in XRD patterns, which suggests the quantities of them are below the resolution of the instrument.

Thermodynamic analyses

It is clear from the aforementioned results that two former exothermic peaks in the DSC curve can be considered as a big exothermic peak, which was interrupted by the melting of Al. Because the exothermic reaction began before the melting of Al, but the reaction rate was slow and the heat was consumed by the melting of Al, the total heat was dropped. On the other hand, the activity of Al increased quickly after Al melted, and the reaction between Ti and Al was promoted. When the heat covered the melting of Al, the second exothermic peak appeared. Therefore, the
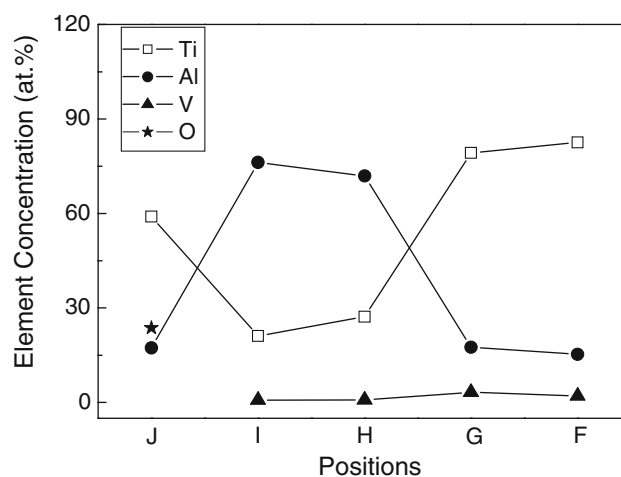


**Fig. 7** Chemical composition of different positions in Fig. 6

exothermic reaction of Ti and Al preceded the melting of Al, and the melting temperature of Al was at about 656 °C.

The possible products at whole temperature range can be evaluated by comparing their free energy change ($\Delta G$). Using thermodynamic data, the $\Delta G$ of Ti–Al intermetallics can be plotted as function of temperature. Figure 9 shows this relationship between $\Delta G$ and temperature, $\Delta G$ curves for $TiAl_2$ and $Ti_2Al_5$ are lower than others, but the formation of them is based on the formed TiAl [16]. Both $\Delta G$ curves for $Ti_3Al$ and TiAl are straight lines, but they have different sloping ratio so that a cross point can be appeared (the cross point at about 700 K). $\Delta G$ of $TiAl_3$ is more negative than $Ti_3Al$ and TiAl in the temperature range of 200–1600 K, indicating that the formation of $TiAl_3$ is easier than direct formation of $Ti_3Al$ and TiAl. Thus, the product at 660 °C was $TiAl_3$.

The third broad exothermic peak (at about 950 °C) shown by the DSC curve is possible due to the formation of multiphase products (Ti–Al compounds), and the formation of oxidation.
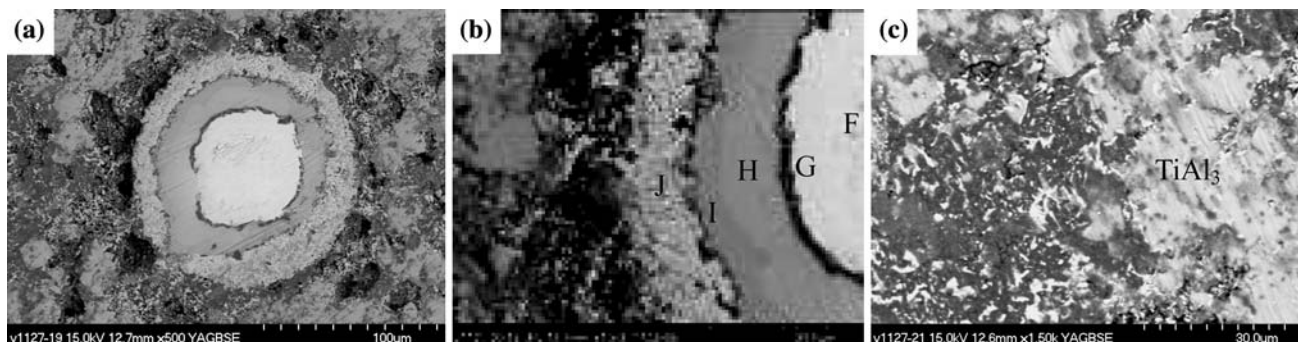


**Fig. 6** SEM micrograph of in situ reaction composites at 1300 °C. **a** Low magnification of Ti fiber and the matrix, **b** high magnification of Ti fiber, **c** high magnification of the matrix
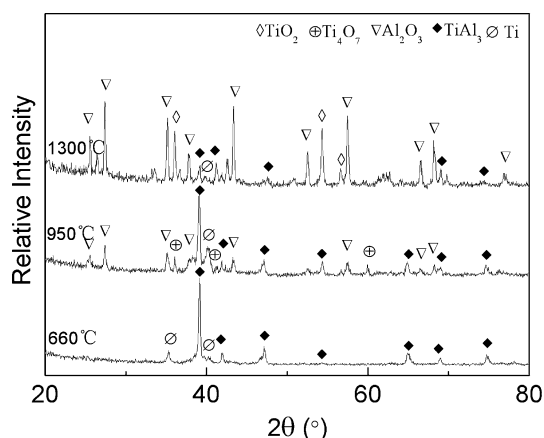
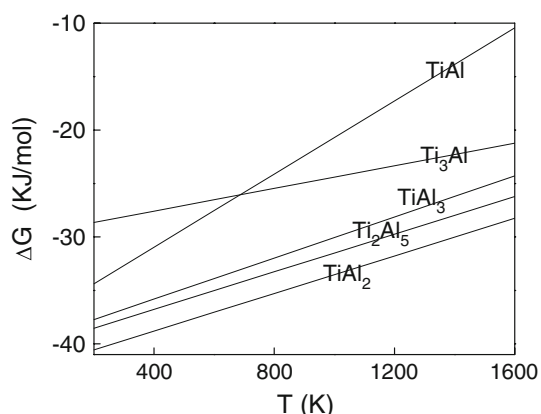**Fig. 8** XRD patterns of in situ reaction composites



**Fig. 9** Free energy changed by temperature of Ti–Al intermetallic compounds

$TiAl_3$ was the unique product between Ti particle and Al. While multiphase products of Ti–Al compounds were formed between Ti fiber and Al. The possible reaction between Ti fiber and Al is shown below.

$$Ti + 3Al = TiAl_3 \qquad (1)$$

$$4Ti + TiAl_3 = Ti_3Al + 2TiAl \qquad (2)$$

$$Ti + Al = TiAl \qquad (3)$$

$$3Ti + Al = Ti_3Al \qquad (4)$$

$$2Ti + Al = Ti_2Al \qquad (5)$$

According to Kattner [17], $\Delta G$ for reaction 2 is that $\Delta G < 0$, and the reaction can proceed.

The different products between two couples (Ti fiber and Al couple, Ti particle and Al couple), it is related to the content of Al in different parts. For Ti particle and Al couple, the amount of Al was high, Al diffused continuously along the grain boundaries of $TiAl_3$ and to be reaction interface, and reaction 1 proceeded constantly, therefore, $TiAl_3$ was the unique product. For Ti fiber and

Al couple, the amount of Al around Ti fiber was limited, Al was consumed soon and reaction 2 began. Al in $TiAl_3$ is a very active element, it diffused along grain boundaries and formed $Ti_xAl_{1-x}$ ($0.25 < x < 0.75$) compounds [18]. In addition, because of O existence, $Al_2O_3$ and $Ti_4O_7$ were detected.

When the temperature reached 1300 °C, the temperature at the reactive interface rose over the melting point of $TiAl_3$ (1390 °C), due to high exothermic heat [19], and local $TiAl_3$ phases melted, leading to islands of $TiAl_3$ existence in the matrix.

Accompanied with $TiAl_3$ decomposition, some rod-shaped products formed. EDX reveals that these were Ti and Al oxides, which were detected as $TiO_2$ and $Al_2O_3$ by XRD. The microstructure and composition of oxidation products are very complex and the reader is referred to previous publications for a more detailed description [20–22]. Since endothermic heat of $TiAl_3$ decomposition is smaller than exothermic heat of oxidation formation, the fourth sharp exothermic peak is owing to the formation of $Al_2O_3$ and $TiO_2$.

Combining both metallographical and thermoanalytical results, the possible reaction mechanism of Ti fiber reinforced $TiAl_3$ composite could be separated into three stages.

First stage, $TiAl_3$ is generated. Below and at the melting point of Al, the product of Ti fiber and Al couple and the product of Ti particle and Al couple are $TiAl_3$.

Second stage, Ti–Al compounds are formed. With the increasing temperature, the content of $Ti_xAl_{1-x}$ ($0.25 < x < 0.75$) will be rearranged according to phase equilibrium through elements diffusion.
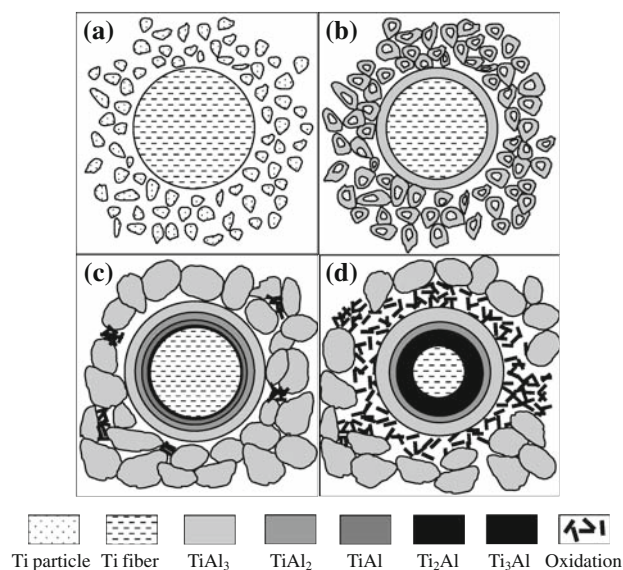


**Fig. 10** A model for the infiltration-in situ reaction mechanism of Ti fiber reinforced $TiAl_3$ composites. **a** reactants, **b** forming $TiAl_3$, **c** forming multiphase Ti–Al compounds, **d** decomposing $TiAl_3$ and forming oxidation

Last stage, $TiAl_3$ decomposes and oxidation occurs. $TiAl_3$ is an unstable phase at higher temperature, accompany with the decomposition of $TiAl_3$, $TiO_2$, and $Al_2O_3$ are formed.

A model of the infiltration-in situ reaction mechanism of Ti fiber reinforced $TiAl_3$ composite is shown in Fig. 10.

## Conclusions

The reaction product between Ti particle and Al was $TiAl_3$ under a particular range of holding temperature. $TiAl_3$ decomposed when reaction temperature at 1300 °C.

The reaction product between Ti fiber and Al were complex. $TiAl_3$ was formed at Ti fiber and Al interface initially, when the as-cast material was heated to 950 °C, multiphase Ti–Al compounds were formed due to interaction between Ti and $TiAl_3$.

At high temperature (>950 °C) oxidation occurred. $Al_2O_3$, $Ti_4O_7$, and $TiO_2$ were formed.

Ti fiber reinforced $TiAl_3$ composite has been prepared by infiltration-in situ reaction. The reaction among Ti fiber, Al, and Ti particle can be separated into three stages: $TiAl_3$ generated and formed a layer; multiphase Ti–Al compounds formed; $TiAl_3$ decomposed, and oxidation occurred.

## References

1. Clemens H, Kestler H (2000) Adv Eng Mater 2:551
2. Wu XH (2006) Intermetallics 14:1114
3. Djanarthany S, Viala J-C, Bouix J (2001) Mater Chem Phys 72:301
4. Colinet C, Pasturel A (2002) Intermetallics 10:751
5. Wang T, Zhang JS (2006) Mater Chem Phys 99:20
6. Milman YV, Miracle DB, Chugunova SI, Voskoboinik IV, Korzhova NP, Legkaya TN, Podrezov YN (2001) Intermetallics 9:839
7. Hsu CJ, Chang CY, Kao PW, Ho NJ, Chang CP (2006) Acta Mater 54:5241
8. Prakash U, Buckley RA, Jones H, Sellars CM (1992) J Mater Sci 27:2001. doi:10.1007/BF01117910
9. Kiyoshi M, Kanryu I, Masami S, Masao I, Masakazu K, Isamu Y (2006) Mater Sci Eng A 428:175
10. Mileiko ST, Povarova KB, Korzhov VP, Serebryakov AV, Kolchin AA, Kiiko VM, Starostin MY, Sarkissyan NS, Antonova AV (2001) Scripta Mater 44:2463
11. Sanguinetti Ferreira RA, Arvieu C, Quenisset JM (2005) Scripta Mater 53:329
12. Sanguinetti Ferreira RA, Arvieu C, Guillaume B, Quenisset JM (2006) Composites Part A 37:1831
13. Lü XH, Yang YQ, Ma ZJ, Liu CX, Chen Y (2006) Trans Nonferrous Met Soc China 16:77
14. Zhang QC, He GY, Wu JS (2000) Mater Sci Technol 8(4):77
15. He GY, Hu SP, Chu SJ, Li LF, Zhang TX, Cai XZ (1996) Chin J Nonferrous Met 6(4):110
16. Mark A, Didier de F (1992) Phys Rev B 46(9):5055
17. Kattner UR, Lin JC, Chang YA (1992) Metall Trans 23A:2081
18. Liu Y, Huang BY, He YH (2000) Trans Nonferrous Met Soc China 10(1):29
19. Jinkeun O, Sung G, Sunghak L, Nack JK (2003) J Mater Sci 38:3647. doi:10.1023/A:1025637600400
20. Kovács K, Perczel IV, Josepovits VK, Kiss G, Réti F, Deák P (2002) Appl Surf Sci 200:185
21. Camille YJ, William EL, Evan C (2006) Intermetallics 14:54
22. Zollinger J, Lapin J, Daloz D, Combeau H (2007) Intermetallics 15:1343